applied sciences

MDPI

Article

Comparison of 2- and 3-Dimensional Cultured Periodontal Ligament Stem Cells; a Pilot Study

Yun Yeong Jeong [1], Mi Sun Kim [2], Ko Eun Lee [3], Ok Hyung Nam [2], Ji-Hyun Jang [4], Sung-Chul Choi [2] and Hyo-Seol Lee [2,*]

1 Department of Pediatric Dentistry, Graduate School, Kyung Hee University, Seoul 02447, Korea; pp5049@naver.com
2 Department of Pediatric Dentistry, School of Dentistry, Kyung Hee University, Seoul 02447, Korea; pedokms@khu.ac.kr (M.S.K.); pedokhyung@khu.ac.kr (O.H.N.); pedochoi@khu.ac.kr (S.-C.C.)
3 Department of Pediatric Dentistry, Kyung Hee University Dental Hospital, Seoul 02447, Korea; olivedlr@naver.com
4 Department of Conservative Dentistry, Kyung Hee University School of Dentistry, Seoul 02447, Korea; jangjihyun@khu.ac.kr
* Correspondence: snowlee@khu.ac.kr; Tel.: +82-2-958-9363

Abstract: This study compared the characteristics of periodontal ligament stem cells (PDLSCs) cultured using 3-dimensional (3D) versus conventional 2-dimensional (2D) methods. PDLSCs were cultured in either a 3D culture with a non-adhesive culture plate (Stemfit 3D®) or a conventional 2D culture using a 6-well plate. Morphology, viability, proliferation ability, and osteogenic differentiation were analyzed to characterize the differences induced in identical PDLSCs by 3D and 2D culture environments. In addition, gene expression was analyzed using RNA sequencing to further characterize the functional differences. The diameter and the viability of the 3D-cultured PDLSCs decreased over time, but the shape of the spheroid was maintained for 20 days. Although osteogenic differentiation occurred in both the 2D- and 3D-cultured PDLSCs, compared to the control group it was 20.8 and 1.6 higher in the 3D- and 2D-cultured cells, respectively. RNA sequencing revealed that PDLSCs cultured using 2D and 3D methods have different gene expression profiles. The viability of the 3D-cultured cells was decreased, but they showed superior osteogenic differentiation compared to 2D-cultured cells. Within the limitations of this study, the results demonstrate that the structure and function of PDLSCs are influenced by the cell culture method.

Keywords: periodontal ligament stem cell; 3-dimensional culture; spheroid; morphology; osteogenic differentiation; RNA sequencing

Citation: Jeong, Y.Y.; Kim, M.S.; Lee, K.E.; Nam, O.H.; Jang, J.-H.; Choi, S.-C.; Lee, H.-S. Comparison of 2- and 3-Dimensional Cultured Periodontal Ligament Stem Cells; a Pilot Study. *Appl. Sci.* **2021**, *11*, 1083. https://doi.org/10.3390/app11031083

Received: 22 December 2020
Accepted: 22 January 2021
Published: 25 January 2021

1. Introduction

Mesenchymal stem cells (MSCs) have self-renewal and multilineage differentiation potency. In humans, they can be harvested from various tissues such as bone marrow, adipose tissue, and umbilical cord blood [1]. In addition, they have been successfully extracted from the periodontal ligaments of permanent teeth [2]. Periodontal ligament stem cells (PDLSCs) are easy to obtain, have a greater proliferation rate than bone marrow stem cells, are capable of differentiating into osteoblasts, cementoblasts, adipocytes, and chondrocytes, and can form a structure similar to periodontal ligaments in vitro [3]. In addition, the relationship between periodontitis and a stem cell has been revealed in recent years [4–6].

Cell cultures are essential for the study of MSCs. Conventional cell culture methods are two-dimensional (2D) methods in which cells are cultured on the bottom of a culture-compatible polystyrene plate. Such cultures create an environment for studying biological processes or cell mechanisms under specific experimental conditions and maintain various types of proliferation [7]. However, in nature, cells grow three-dimensionally rather

than in a 2D plane. Therefore, it is difficult to study cell-to-cell signal transduction and the functions of cells in a conventional 2D culture environment [8]. To overcome these limitations, cell research using three-dimensional (3D) culture technology is being actively pursued. Such cultures have the advantage of emulating the original characteristics of the cell's environment so that the cell can display form, function, and activity as close to natural as possible [9,10]. In addition, 3D cell culture has attracted attention because it can function as a substitute for animal experimentation [11].

There are two general methods of 3D cell culture. The first involves creating a scaffold of microstructures the cells can use to move, proliferate, differentiate, and contact each other [11]. However, scaffolds have limitations that can negatively affect cell stability and cell behavior during incubation [12]. In the case of hydrogel among the scaffold techniques, there is also a problem that the hydrogel collapses during the media replacement process [13]. In the scaffold-free method, a pellet or centrifugation tube culture, low-adhesion plate culture, bioreactor, hanging drop culture, or a pellet culture and liquid overlay are used to create 3D microstructures without scaffolding [7,11,12,14]. In these methods, cells assemble an endogenous extracellular matrix to form their own preferred microenvironment [11,15,16].

Cells cultured in a 3D environment behave differently than those in a 2D environment [14]. For example, primary articular chondrocytes and hepatocytes cultured in a 2D environment rapidly lose their normal phenotypes, but in 3D cultures, the normal phenotype is maintained [17]. In addition, 3D-cultured stem cells exhibit better osteoblastic, adipogenic, and neuronal differentiation than 2D-cultured stem cells [15,18,19]. Similarly, 3D-cultured human dental pulp cells show higher expression of osteocalcin, dentin sialophosphoprotein, and alkaline phosphatase than those cultured under 2D conditions [20]. The expression of these proteins is influenced by cell–cell and cell–matrix interactions, which are difficult to imitate in 2D culture. In addition, the expression of multilineage differentiation-related genes, such as Nanog and Oct4, and pluripotency transcription factor-related genes, is higher in 3D-cultured cells than those grown in 2D culture [21]. These studies demonstrate how cell culture conditions can influence gene expression [14,22]. However, because previous studies have usually used microarrays and polymerase chain reaction (PCR), few studies have analyzed genome-wide expression.

This pilot study compared the morphology, viability, stemness, and functional gene expression of PDLSCs cultured using either 3D or conventional 2D methods.

2. Materials and Methods

2.1. 2D and 3D Culture of Human Permanent Periodontal Ligament Stem Cells

Permanent human PDL stem cells were purchased from Cell Engineering for Origin (CEFO Co., Ltd., Seoul, Korea). The cell donor's personal information was not provided and the examination of Institutional Review Board was waived. The cells were cultured in a 37 °C incubator with 5% CO_2 using Dulbecco's modified Eagle's medium (DMEM, Gibco, Waltham, MA, USA) growth media. Low glucose DMEM was used with 10% fetal bovine serum (FBS, Corning Life Sciences, New York, NY, USA) and gentamicin (5 µg/mL, Invitrogen-GIBCO, Carlsbad, CA, USA). After 3–4 passages, the cells were split and thereafter grown under either 2D or 3D conditions.

2.2. Formation of Stem Cell Spheroids through 3D Culture (Stemfit 3D®)

The formation of stem cell spheroids through 3D culture was carried out with 600 µm diameter polydimethylsiloxane-based concave micromolds (Prosys Stemfit 3D®; Prodizen Inc., Seoul, Korea). Seeded in a concave micromold and cultured in a 37 °C incubator with 5% CO_2 using DMEM were 1.2×10^6 cells.

2.3. Morphology

To observe their morphology, 2D-cultured cells and the spheroids formed by the 3D-culture cells were observed on days 1, 3, 5, and 7 under a fluorescent microscope (JuLI,

Nanoentek Inc., Seoul, Korea). In addition, spheroids were observed daily for 10 days to analyze the change in diameter. Additionally, mean diameters of at least 30 spheroids were compared daily. To observe the long-term stability of the spheroids, the cells were monitored for 20 days.

2.4. Viability Analyses Using Cell Counting Kit-8 and LIVE/DEAD Cell Viability Assays

The Cell Counting Kit-8 assay (CCK-8; Dojindo Molecular Technologies, Kumamoto, Japan) and LIVE/DEAD assay (LIVE/DEAD Viability/Cytotoxicity Kit for mammalian cells; Invitrogen, Carlsbad, CA, USA) were used to quantify the cell proliferation ability. The CCK-8 assay is based on the activation of 1-methoxy phenazinium methylsulfate by nicotinamide adenine dinucleotide phosphate (NADP) and nicotinamide adenine dinucleotide phosphate hydrogen (NADPH) produced by dehydrogenase in the metabolism of living cells. Water-soluble tetrazolium salt, 2- (2-methoxy-4-nitrophenyl), -3- (4-nitrophenyl), -5- (2,4-disulfophenyl), -2H tetrazolium, and monosodium salt (WST-8) were reduced to orange formazan, therefore, the amount of WST-8 formazan produced by the dehydrogenase in the cell is directly proportional to the number of viable cells, and the proliferation ability of the cells is quantitatively examined.

The LIVE/DEAD assay quantifies living and dead cells by measuring the esterase activity and plasma membrane integrity of the cells. The non-fluorescent dye, calcein AM, converts to a fluorescent calcein that fluoresces in the presence of esterase in living cells, producing a uniform green fluorescence. Ethidium homodimer-1 enters dead cells through damaged membranes and binds with nucleic acids to produce a red fluorescence.

First, the 2D- and 3D-cultured PDLSCs were seeded at a density of 1.0×10^5 per well on a 6-well plate and subjected to the LIVE/DEAD assay on days 3, 5, and 7. The images were taken with a fluorescence microscope (IX71; Olympus, Tokyo, Japan). Meanwhile, the CCK-8 assay was performed on days 1, 3, 5, and 10, and the absorbance was measured at 450 nm using a Benchmark Plus Multiplate Spectrophotometer (Bio-Rad, Hercules, CA, USA).

2.5. Osteogenic Differentiation

Next, 2D- and 3D-cultured PDLSCs were cultured in osteo-inductive media (osteo group) and basal media (control group) to confirm the ability of PDLSCs to differentiate into bone cells. The osteo group was cultured for 2 weeks in osteo-inductive media with 15% FBS, 250 μL gentamycin reagent solution (final concentration 5 μg/mL), 5 mL L-ascorbic acid (final concentration 10 mM/L), and 5 mL dexamethasone (final concentration 10 mM/L). To evaluate cell differentiation, Alizarin Red S (ARS) staining was performed to visualize calcium formation. Cells were fixed with ice-cold 70% ethanol for 15 min, stained with ARS solution for 3 min, washed, and observed with an optical microscope. For quantitative evaluation of hard tissue formation, 10% cetylpyridinium chloride was added for 10 min and the ARS stain extract was extracted, transferred to a 96-well plate, and its absorbance was measured at a wavelength of 562 nm.

2.6. RNA Expression

2.6.1. RNA Isolation

Then 2D- and 3D-cultured PDLSCs were selected on day 5 for gene expression analyses. The RNA was isolated using RiboEx (GeneAll, Seoul, Korea) and RNA quality was assessed using an Agilent 2100 bioanalyzer with and RNA 6000 Nano Chip (Agilent Technologies, Amstelveen, The Netherlands). RNA quantification was performed using an ND-2000 Spectrophotometer (Thermo Inc., Wilmington, DE, USA).

2.6.2. Library Preparation and Sequencing

Libraries of control and test RNAs were constructed using the QuantSeq 3′ mRNA-Seq Library Prep Kit (Lexogen Inc., Vienna, Austria) according to the manufacturer's instructions. In brief, 500 ng RNA was prepared, hybridized to an oligo-dT primer contain-

ing an Illumina-compatible sequence at its 5′-end, and subjected to reverse transcription. After degradation of the RNA template, second-strand synthesis was initiated using a random primer containing an Illumina-compatible linker sequence at its 5′-end. The double-stranded library was purified using magnetic beads to remove all reaction components. Then the library was amplified to add the complete adapter sequences required for cluster generation. The finished library was purified to remove PCR components. High-throughput sequencing was performed as single-end 75 bp sequencing using a NextSeq 500 sequencer (Illumina Inc., Foster City, CA, USA).

2.6.3. Data Processing for Identification of Differentially Expressed Genes

QuantSeq 3′ mRNA-Seq reads were aligned using Bowtie 2. Bowtie 2 indices were either generated from a genome assembly sequence or the representative transcript sequences for aligning the genome and transcriptome. The alignment file was used to assemble transcripts, estimate their abundances, and detect the differential expression of genes. Differentially expressed genes were identified based on counts from unique and multiple alignments using coverage in BEDtools. The read count data were processed based on the quantile normalization method using EdgeR within R software (R Development Core Team, Vienna, Austria) with a bioconductor.

2.7. Statistical Analyses

Statistical analyses were performed with SPSS (Statistical Package for Social Sciences, version 25.0; IBM Corporation, Armonk, NY, USA). One-way ANOVA and Scheffe post hoc analyses were performed to compare the absorbance of each experimental group. A p-value < 0.05 was considered to indicate statistical significance.

3. Results

3.1. Morphology

PDLSCs grown in 2D cultures expressed a bipolar and stellate form. Cells were attached to the plate and increased in number over time (Figure 1A–D). In the 3D culture, PDLSCs aggregated and became spheroid for about 24 h (Figure 1I,J). Then the diameters of the spheroids significantly decreased by approximately 67.1% until day 5, after which they did not change (Figure 1E–H). After day 13, the shape of the spheroids became increasingly unstable and they subsequently dispersed after day 20 (Figure 1I–P).

3.2. Viability Analyses Using CCK-8 and LIVE/DEAD Cell Viability Assays

The results of the CCK-8 assay showed that the absorbance of 2D-cultured PDLSCs increased significantly from 0.31 to 3.24 over time. In particular, the absorbance increased exponentially on day 10 (p = 0.012). By contrast, the absorbance of 3D-cultured PDLSCs continued to decrease over time from 0.52 to 0.32 (Figure 2). This decrease was significant from days 1 to 5 (p = 0.043) but the decrease was not significant between days 5–10 (p = 0.242).

The results of the LIVE/DEAD assay revealed that the 2D-cultured PDLSCs did not show a significant increase in dead cells, however, a cavitation of cells was observed in the center of the spheroids in the 3D culture (Figure 3).

3.3. Stemness and Osteogenic Differentiation

ARS staining revealed significant extracellular calcium deposits in both the 2D and 3D cultures, which is indicative of osteogenic differentiation (Figure 4). Compared to the control group, the absorbance of the ARS stain extract was 20.8 and 1.6 times higher in the 3D and 2D cultures, respectively (Figure 5). There was a significant statistical difference in 3D culture (p = 0.06).

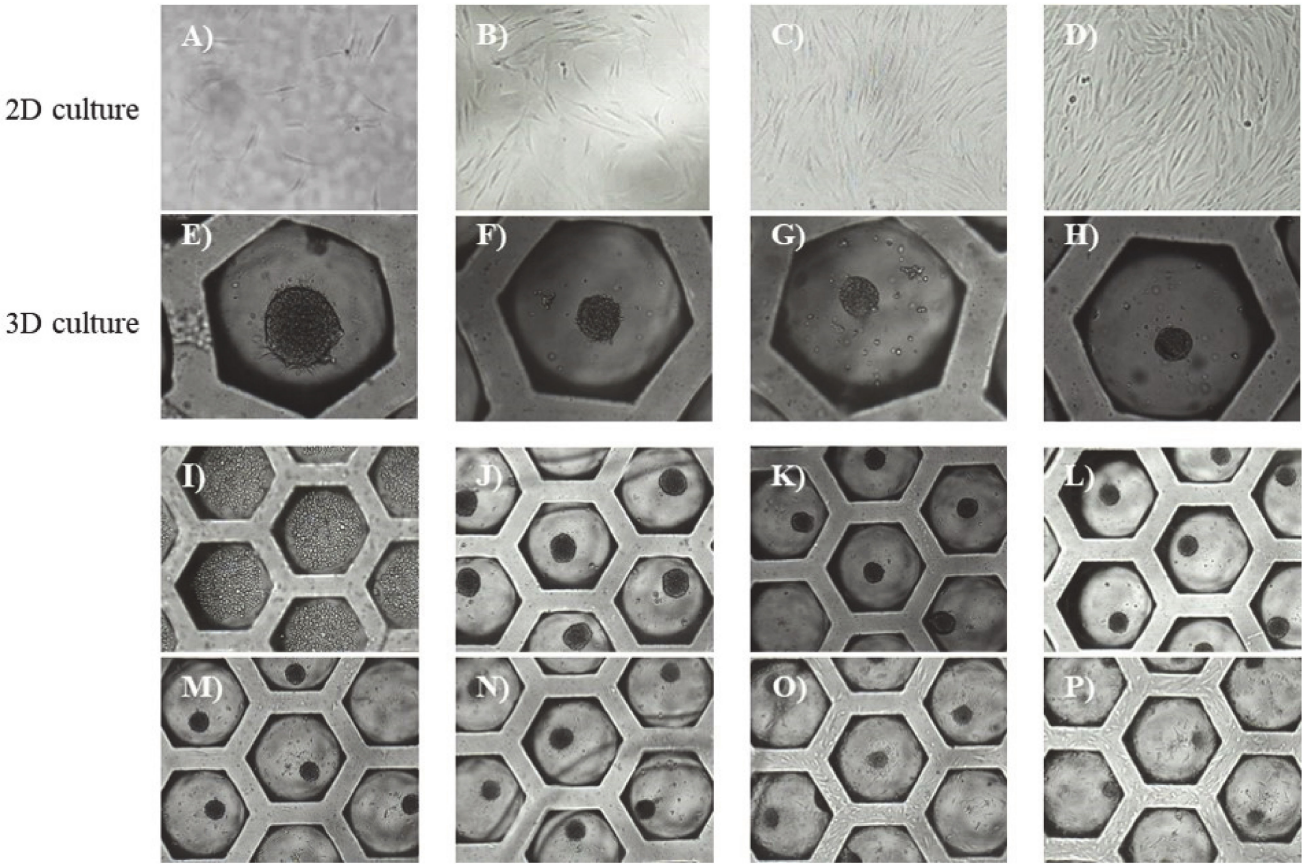

Figure 1. Morphology, day 1–20. (**A**–**H**) Cell morphology of the periodontal ligament stem cell (PDLSC) at days 1, 3, 5, and 7 in 2D and 3D culture (magnification, ×200). (**I**–**P**) Morphology of the PDLSC spheroids at days 0, 1, 3, 5, 7, 9, 13, and 20 (magnification, ×100). At day 13, the spheroids began to collapse, but the shape of spheroids remained relatively stable until day 20.

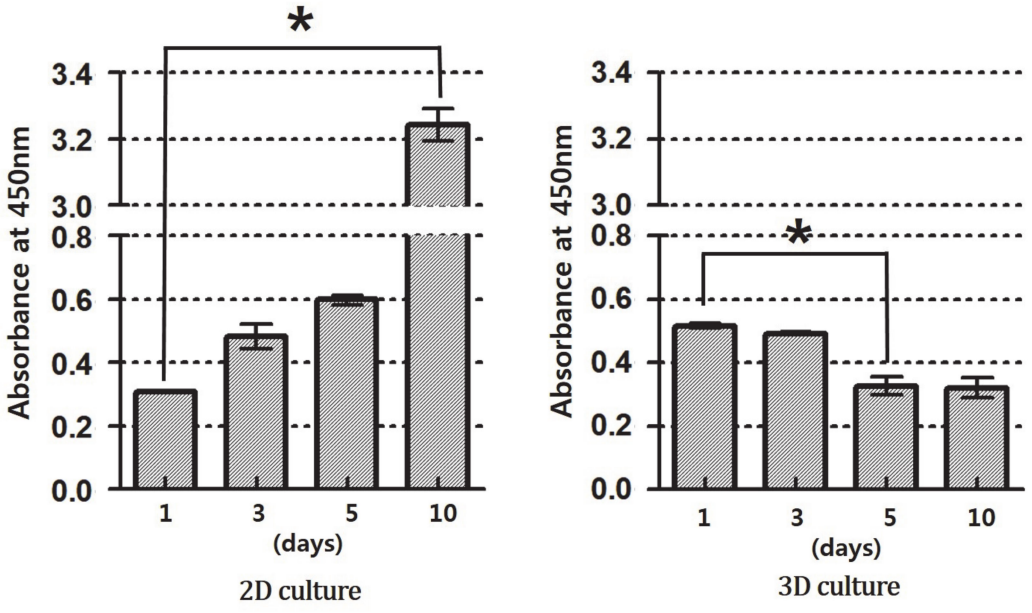

Figure 2. Results of the CCK-8 assay. 2D-cultured PDLSCs showed an increase in absorbance while the 3D-cultured PDLSCs showed a significant decrease in absorbance from day 1 to 5. * $p < 0.05$ comparison of absorbance; Schaffe's post hoc test following one-way ANOVA.

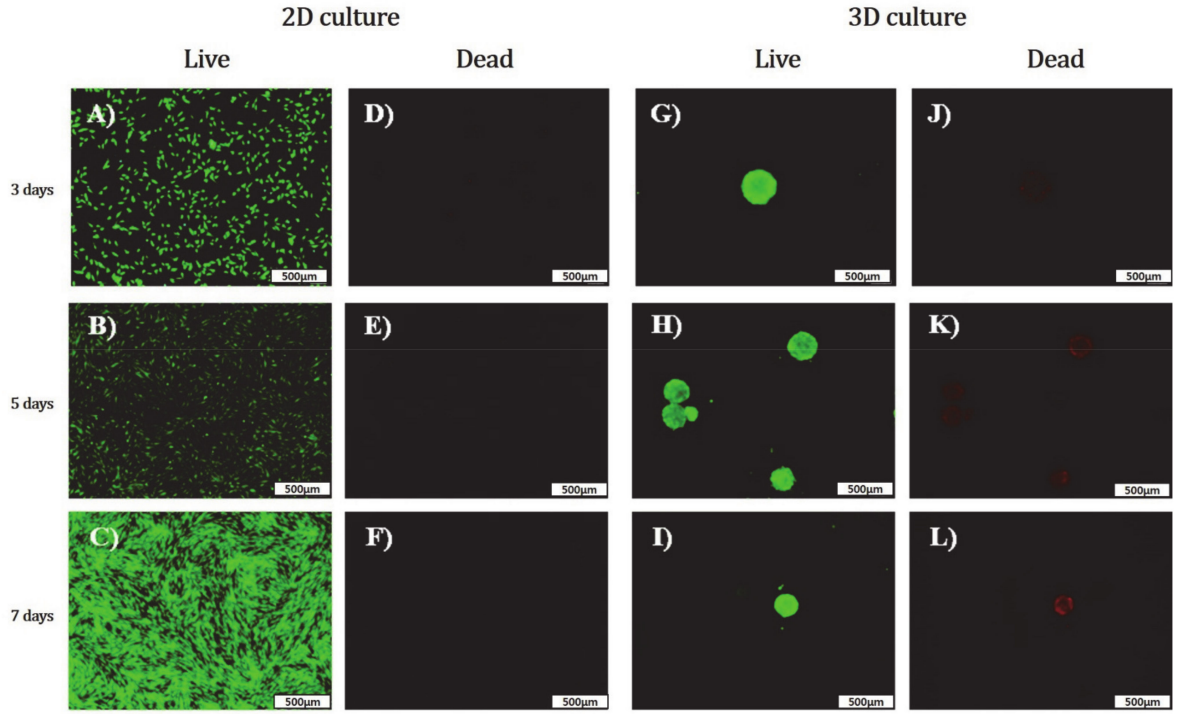

Figure 3. Results of the LIVE/DEAD assay. (**A**–**F**) LIVE/DEAD assay results for 2D-cultured PDLSCs at days 3, 5, and 7 (magnification, ×100). The number of cells increased and no dead cells were observed. (**G**–**L**) LIVE/DEAD assay results for 3D-cultured PDLSCs at days 3, 5, and 7 (magnification, ×100). 2D-cultured PDLSCs did not show a significant increase in dead cells, however, a cavitation of cells was observed in the center of the spheroids in the 3D culture.

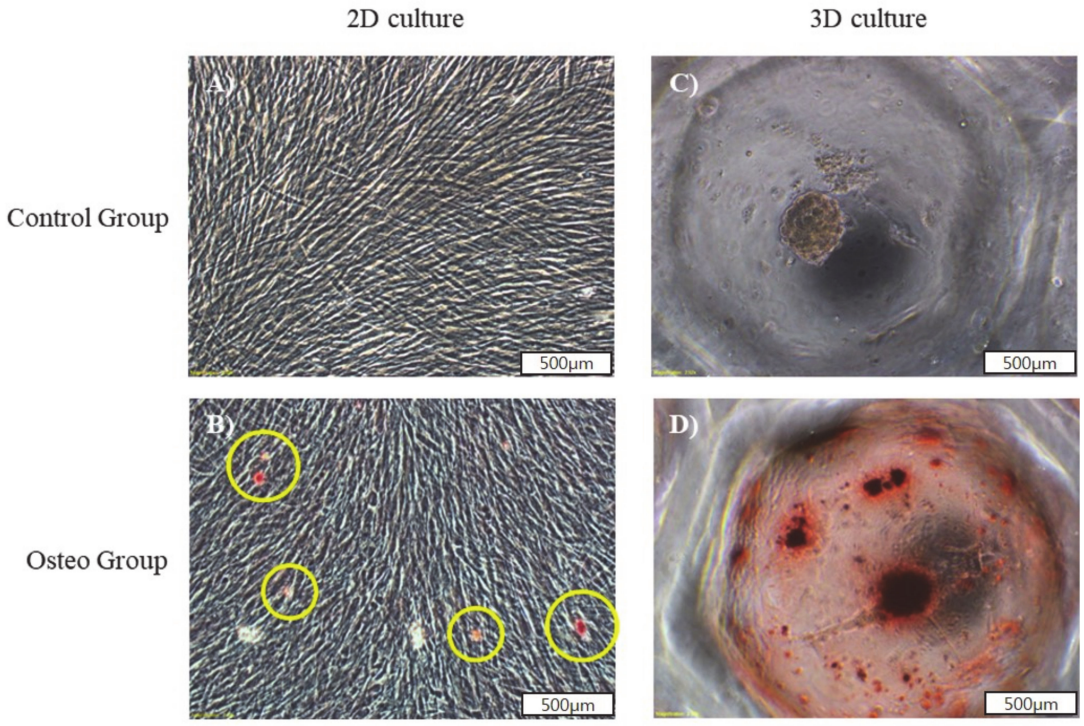

Figure 4. Evaluation of osteogenesis in 2D- and 3D-cultured PDLSCs (magnification, ×200). (**A**) Control group of 2D-cultured PDLSCs in basal media. (**B**) Osteo group of 2D-cultured PDLSCs in osteogenic media. (**C**) Control group of 3D-cultured PDLSCs in basal media. (**D**) Osteo group of 3D-cultured PDLSCs in osteogenic media.

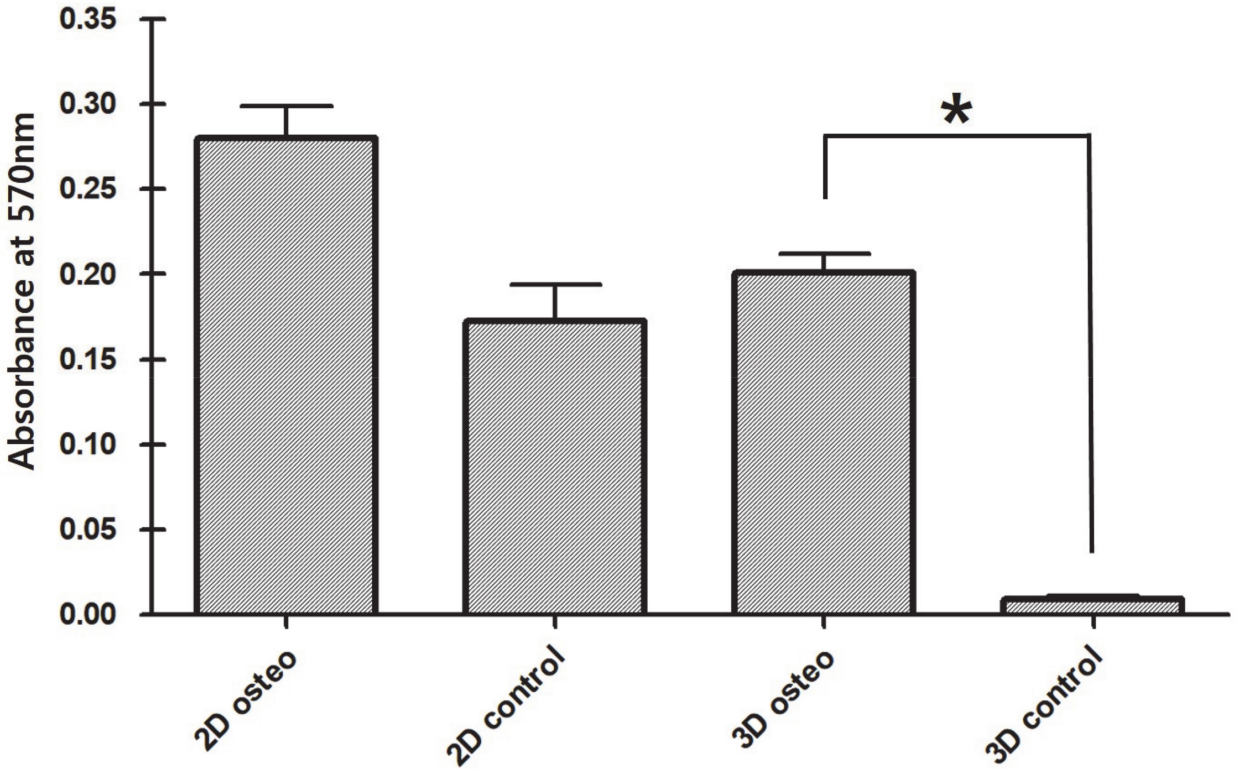

Figure 5. Result of alizarin red S staining of PDLSCs on the 14th day. In the 2D-cultured cells, the absorbance was 1.6 times higher in the osteo group than in the control group. In the 3D-cultured cells, the absorbance was 20.8 times higher in the osteo group than in the control group. * $p < 0.05$ comparison with the control group; Schaffe's post hoc test following one-way ANOVA.

3.4. Identification of Differentially Expressed Genes and Gene Ontology Analyses

The expression levels of 25,737 differentially expressed genes in the 2D- and 3D-cultured PDLSCs were examined. Of these, 5664 genes related to cell function, immunity, inflammation, and the extracellular matrix were selected for further analyses. In the 3D culture, the expression of 214 genes (46.6%) was upregulated and 245 (53.4%) genes were downregulated compared to the 2D culture. Up- or downregulated genes were marked in extracellular matrix (ECM) (16.7%), angiogenesis (15.5%), inflammatory response (13.6%), cell migration (12.2%), and cell proliferation (11.4%). Genes in the 3D-cultured PDLSCs that showed at least a 50-fold increase or decrease compared to the 2D-cultured PDLSCs are presented in Tables 1 and 2.

Table 1. List of genes upregulated more than fifty-fold in 3D-cultured PDLSCs compared to 2D-cultured PDLSCs.

Gene Name	Fold Change	Description	Related Function
MMP1	932.4	matrix metallopeptidase 1	Cell migration, extracellular matrix
SMOC1	525.5	SPARC related modular calcium binding 1	Extracellular matrix
CXCL8	276.1	C-X-C motif chemokine ligand 8	Angiogenesis, cell cycle, cell migration, immune response, inflammatory response
MMP10	190.8	matrix metallopeptidase 10	Extracellular matrix
CXCL1	173.7	C-X-C motif chemokine ligand 1	Cell migration, cell proliferation, immune response, inflammatory response

Table 1. *Cont.*

Gene Name	Fold Change	Description	Related Function
EREG	169.3	epiregulin	Angiogenesis, cell cycle, cell differentiation, cell proliferation
AREG	167.8	amphiregulin	Cell differentiation, cell proliferation
CSF3	159.6	colony stimulating factor 3	Cell differentiation, immune response
TAC1	136.1	tachykinin precursor 1	Immune response, inflammatory response
IER3	125.0	immediate early response 3	Apoptotic process, cell death
COMP	117.5	cartilage oligomeric matrix protein	Apoptotic process, cell death, extracellular matrix
S100A8	110.7	S100 calcium binding protein A8	Apoptotic process, cell death, cell differentiation, cell migration, immune response, inflammatory response
CXCL3	87.3	C-X-C motif chemokine ligand 3	Cell migration, immune response, inflammatory response
C3	86.3	complement component 3	Immune response, inflammatory response
LRP4	84.2	LDL receptor related protein 4	Cell differentiation
PTGS2	83.4	prostaglandin-endoperoxide synthase 2	Angiogenesis, cell differentiation, inflammatory response
SPON1	80.9	spondin 1	Extracellular matrix
COL5A3	73.4	collagen type V alpha 3	Extracellular matrix
PTPN22	69.5	protein tyrosine phosphatase, non-receptor type 22	Cell differentiation
IL24	67.2	interleukin 24	Apoptotic process, cell death
TNFAIP6	65.9	TNF alpha induced protein 6	Immune response, inflammatory response
CYP7B1	64.1	cytochrome P450 family 7 subfamily B member 1	Cell migration
PRDM1	63.7	PR domain 1	Cell differentiation, cell proliferation, immune response
STC1	53.3	stanniocalcin 1	Cell differentiation, cell proliferation

Table 2. List of genes downregulated more than fifty-fold in 3D-cultured PDLSCs compared to 2D-cultured PDLSCs.

Gene Name	Fold Change	Description	Related Function
RSPO2	152.7	R-spondin 2	Cell differentiation
DCLK1	86.8	doublecortin such as kinase 1	Cell differentiation, cell migration
CXCL14	73.9	C-X-C motif chemokine ligand 14	Cell migration, immune response
SEMA3D	65.6	semaphorin 3D	Cell differentiation
TENM2	64.3	teneurin transmembrane protein 2	Cell differentiation
ADRA1B	58.2	adrenoceptor alpha 1B	Cell proliferation

4. Discussion

A scaffold-free 3D culture method, Stemfit 3D®, was used for the 3D culture of PDLSCs and compared to traditional 2D-cultured PDLSCs. The morphology, viability, proliferation ability, differentiation ability, and gene expression of the two groups were analyzed, and it was confirmed that they have different functions and characteristics depending on the culture method although the cells are of the same origin. The viability of the 3D-cultured

cells was decreased, but they showed superior osteogenic differentiation compared to 2D-cultured cells. Additionally, the function of PDLSCs differed by the cell culture method.

Stemfit 3D® utilizes a non-adhesive plate with a 600 µm diameter polydimethylsiloxane-based concave micromold. The reason for using concave micromolds is that they more rapidly aggregate the cells than other methods (plane and cylindrical), and the cells form spheroids that are highly uniform size and easily harvested [23]. Due to its economy and ease of use, Stemfit 3D is commonly used in stem cell cytology and various other cellular studies [24–28].

PDLSC spheroids from 3D cultures showed a rapid decrease (67.1%) in diameter over the first 5 days, followed by a moderate decrease after day 5 (Figure 1E–H). These results indicate that the initial reduction in diameter was due to cell aggregation and organization, but the subsequent reduction appears to be due to restricted nutrients and oxygen. Several models for the transport of nutrients, oxygen, and waste in spheroids have been verified [29–31]. When the diffusion of oxygen is limited, avascular tissue forms, and inefficient transport results in the accumulation of metabolic waste and the formation of a necrotic core at the center of the spheroid [14,16,30,31]. Several studies on MSC spheroids, including Cornelia et al. [15] who studied human MSCs and Yamaguchi et al. [32] who studied rat MSCs, have reported that spheroids form within 1 day and their diameters decrease with time [22,23,28,33,34]. On the other hand, Lee et al. reported that the diameter of human dental pulp stem cell spheroids cultured using a 6-well non-adhesive plate increase over time [21]. This discrepancy is due to the different culture methods used in the studies. Cornelia et al. and Yamaguchi et al. independently cultured MSCs in a small volume of media or used the scaffold method, whereas Lee et al. [21] used a relatively large volume of media. It is possible that spheroid–spheroid interactions may increase the diameter of the spheroids, but further study is needed.

Many previous studies on the morphology of spheroids have only made short-term observations of about 5–7 days [15,22,23,28,33,34]. In 2016, Bellotti et al. [35] used a pellet culture method to study the morphology of human MSC spheroids and found that the diameter of the spheroids decreased rapidly over a 14-day period, after which it remained constant for 2 months. In general, depending on the culture method, the morphology of the spheroids is maintained for 3–21 days and the internal structure is homogeneous and biologically stable for at least 1 month [35,36]. In this study, the spheroids were observed for 20 days to confirm their long-term stability. In addition to the decrease in diameter, the surface integrity of the spheroids began to diminish on day 13 but the shape of the spheroids remained stable (Figure 1I–P). It has been found that 3D culture methods using low-adhesive plates have a lower long-term stability than other methods because of the difficulty limiting the size of the spheroids [36]. However, because Stemfit 3D can control the size of the spheroids, it shows improved stability over a longer period. Further research is needed to determine whether the internal structure and function of cells cultured using the Stemfit 3D system are equally stable in the long-term.

CCK-8 and LIVE/DEAD assays were used to confirm the proliferation ability and viability of 3D-cultured PDLSCs, which are frequently used methods in 2D culture experiments [37–40]. The CCK-8 assay revealed that the absorbance in the 2D culture increased over time while in the 3D culture it decreased over time. This is probably due to the continued proliferation of cells in the 2D environment, while in the 3D environment, the differentiation rate decreased due to the inevitable restriction of nutrients and oxygen in the center of the spheroids (Figure 2) [14,24,25,35]. In addition, in the 3D culture, the LIVE/DEAD assay results showed that the number of dead cells increased over time in the center of the spheroids (Figure 3). Similar results were seen in a previous study of human MSCs grown via pellet culture, where the spheroids maintained a stable internal structure for 1 month, however at 2 months, a necrotic area developed in the center of spheroid, together with a loss of proliferation, impaired structural stability, and decreased cell-to-cell contact [35]. Although quantitative evaluation of 2D- and 3D-culture methods is

difficult [7], these results are significant because it supports the idea that the characteristics of the 3D-cultured cells are fundamentally different from the 2D-cultured cells.

One of the benefits of 3D culture is it improves osteogenic differentiation compared to 2D culture. In addition, studies about the differentiation potential of stem cells have shown that the intercellular interactions in embryonic stem cells are better expressed in a 3D environment [14,34,41]. For example, salivary-gland-derived progenitor cells can differentiate into hepatocytic and pancreatic islet cell lineages only when cultured in a 3D culture environment [42]. For this reason, 3D culture has attracted attention in stem cell biology and oncology, and in 3D-culture studies on dental stem cells [8,14]. For example, 3D-cultured dental pulp stem cells or gingiva/papilla-derived stem cells show higher ALP activity than those grown in 2D culture [26–28]. In addition, the expression of genes associated with bone formation, such as BMP2, RUNX2, and dentine sialophosphoprotein (DSPP), are also highly expressed in these 3D-cultured cells [21,32]. In this experiment, both 2D- and 3D-cultured PDLSCs showed osteo-differentiation. However, compared to the control group, ARS staining showed that the 3D-cultured PDLSCs had significantly higher absorbance than the 2D-cultured PDLSCs (20.8 and 1.6 times higher, respectively). This suggests that more mineralized tissue is produced by the 3D-cultured PDLSCs compared to their 2D counterparts [21].

RNA sequencing was used to analyze the gene expression profiles of PDSLCs grown in 2D and 3D culture environments. In previous studies, such gene expression profiles have been analyzed via a microarray or PCR, but both of these methods are limited by the fact that only selected genes can be identified. Since RNA sequencing can capture a wider range of active genes, it is possible to detect small changes in expression with a limited amount of transcripts [43].

In this study, RNA sequencing results showed that the expression of genes related to the ECM, angiogenesis, and inflammation, such as MMP1, SMOC1, MMP10, CXCL8, CXCL1, and EREG, was very high. Previously, 3D-cultured MSCs have been shown to display increased expression of genes related to angiogenesis, inflammation, and proliferation, such as TGS-6, IL24, VEGF, FGF-2, CXCR4, MCP3, RANTES, EGF, and SDF [36]. The increased expression of angiogenic genes is evidenced by the observation that 3D-cultured MSCs demonstrate more potent angiogenic effects than 2D-cultured MSCs, which allows them to restore more tissue than their 2D counterparts [44]. In addition, 3D-cultured MSCs show increased expression of osteogenic- and adipogenic-related genes, such as RUNX-2, OXC, OC, OPN, COLI, OCN, DDPP, DMP1, LPL, FABP4, PLN4, and PPARr [21,32–34,45]. These genes promote adipogenic and osteogenic differentiation by increasing the production of ECM proteins and endogenous growth factors [36].

The initial coalescence of the spheroids is caused by caspase-dependent IL1 autocrine signaling, which upregulates EGR2 [22]. It is noteworthy that this study did not show any significant difference in the expression of EGR2, however, the expression of EGR1 and EGR3 were increased 4.90 and 5.57 fold, respectively. Similarly, immunomodulatory mediators such as IL6 (2.07 fold) and TNFAIP6 (65.87 fold) and chemokine receptors such as CXCR4 (3.96 fold) were upregulated in response to IL1 autocrine signaling in the 3D spheroids [46,47]. A previous study found that in the center of the spheroids, where the apoptosis zone is formed due to the restriction of nutrients and oxygen, hypoxia- and apoptosis-related genes such as VEGFA and hypoxia inducible factor (HIF) are also upregulated [14]. In this study, hypoxia-associated genes such as HIF1A and HIF3A and apoptosis-related genes such as IER3, COMP, and S100A8 were highly upregulated in the spheroids, while the expression of genes related to cell differentiation and proliferation such as RSPO2, DCLK1, and CXCL14 were highly downregulated. These results are consistent with the observation that over time, the apoptotic zone of the spheroid increases and the surface proliferation zone decreases.

This study had several limitations. First, the decreased diameter and reduced proliferation ability of the 3D-cultured PDLSCs may be due to inherent characteristics of the PDLSCs or may be attributed to the morphologic characteristics of the spheroid, which make it

difficult to supply adequate nutrients and oxygen and discharge waste products. Results of this study are similar to other studies that have used 3D pellet cultures, low-adhesive plates, or scaffolds. In this regard, it may be necessary to compare other 3D methods, such as a bioreactor. Second, the assays that were optimized for a 2D environment may not have been optimal for evaluating 3D-cultured cells. For example, the CCK-8 assay is a method of measuring the color change caused by the dehydrogenation of water-soluble tetrazolium salts by living cells [37]. Therefore, it is not ideal to compare the absorbance of 2D and 3D cultures quantitatively because the number of cells contacting the solution differs between the culture environments. It is difficult or impossible to find protocols and assays optimized for 3D-cultured PDLSCs, and therefore in conjunction with the increasing popularity of 3D culture, future research is necessary to establish optimized methods for analyzing 3D-cultured cells. Third, this was a pilot study for comparing 2D- and 3D-cultured PDLSCs, and as such, it had a limited sample size. Despite these limitations, it confirmed that the 3D-cultured PDLSCs display different gene expression, morphology, and physiology compared to identical 2D-cultured cells. Moreover, the results of this study will contribute to developing optimized 3D-culture methods for dental stem cells.

5. Conclusions

The viability of the 3D-cultured cells was decreased, but they showed superior osteogenic differentiation compared to 2D-cultured cells. Within the limits of this study, it confirmed that the gene expression, function, differentiation, and proliferation of identical stem cells differ depending on the culture method. However, it was difficult to quantitatively compare 2D and 3D culture using conventional analytical methods optimized for 2D culture. Therefore, further studies are necessary to develop standard processes and analytical methods for cells cultured in a 3D environment.

Author Contributions: Conceptualization, Y.Y.J. and H.-S.L.; methodology, J.-H.J.; software, M.S.K.; validation, Y.Y.J., H.-S.L. and J.-H.J.; formal analysis, K.L.; investigation, O.H.N.; resources, S.-C.C.; data curation, Y.Y.J.; writing—original draft preparation, Y.Y.J. and H.-S.L.; writing—review and editing, M.S.K., K.L., O.H.N., J.-H.J. and S.-C.C.; visualization, Y.Y.J.; supervision, H.-S.L.; project administration, H.-S.L.; funding acquisition, H.-S.L. All authors have read and agreed to the published version of the manuscript.

Funding: This research was supported by the Bio & Medical Technology Development Program of the National Research Foundation of Korea (NRF-No.2019R1G1A1100082) and by the Basic Science Research Program of the NRF (NRF- 2020R1C1C1006937) funded by the Ministry of Education, Science, and Technology.

Institutional Review Board Statement: Not applicable.

Informed Consent Statement: Not applicable.

Data Availability Statement: The data presented in this study are openly available.

Acknowledgments: Thanks to everyone helped in this study.

Conflicts of Interest: The authors declare no conflict of interest.

References

1. Jin, H.J.; Bae, Y.K.; Kim, M.; Kwon, S.J.; Jeon, H.B.; Choi, S.J.; Kim, S.W.; Yang, Y.S.; Oh, W.; Chang, J.W. Comparative analysis of human mesenchymal stem cells from bone marrow, adipose tissue, and umbilical cord blood as sources of cell therapy. *Int. J. Mol. Sci.* **2013**, *14*, 17986–18001. [CrossRef] [PubMed]
2. Seo, B.M.; Miura, M.; Gronthos, S.; Bartold, P.M.; Batouli, S.; Brahim, J.; Young, M.; Robey, P.G.; Wang, C.Y.; Shi, S. Investigation of multipotent postnatal stem cells from human periodontal ligament. *Lancet* **2004**, *364*, 149–155. [CrossRef]
3. Saito, M.T.; Silverio, K.G.; Casati, M.Z.; Sallum, E.A.; Nociti, F.H., Jr. Tooth-derived stem cells: Update and perspectives. *World J. Stem Cells* **2015**, *7*, 399–407. [CrossRef] [PubMed]
4. Isola, G.; Lo Giudice, A.; Polizzi, A.; Alibrandi, A.; Murabito, P.; Indelicato, F. Identification of the different salivary Interleukin-6 profiles in patients with periodontitis: A cross-sectional study. *Arch. Oral Biol.* **2020**, *122*, 104997. [CrossRef] [PubMed]

5. Isola, G.; Polizzi, A.; Alibrandi, A.; Williams, R.C.; Leonardi, R. Independent impact of periodontitis and cardiovascular disease on elevated soluble urokinase-type plasminogen activator receptor (suPAR) levels. *J. Periodontol.* 2020. [CrossRef]
6. Isola, G.; Polizzi, A.; Patini, R.; Ferlito, S.; Alibrandi, A.; Palazzo, G. Association among serum and salivary A. actinomycetem-comitans specific immunoglobulin antibodies and periodontitis. *BMC Oral Health* **2020**, *20*, 283. [CrossRef]
7. Fennema, E.; Rivron, N.; Rouwkema, J.; van Blitterswijk, C.; de Boer, J. Spheroid culture as a tool for creating 3D complex tissues. *Trends Biotechnol.* **2013**, *31*, 108–115. [CrossRef]
8. Knight, E.; Przyborski, S. Advances in 3D cell culture technologies enabling tissue-like structures to be created in vitro. *J. Anat.* **2015**, *227*, 746–756. [CrossRef]
9. Rossi, M.I.; Barros, A.P.; Baptista, L.S.; Garzoni, L.R.; Meirelles, M.N.; Takiya, C.M.; Pascarelli, B.M.; Dutra, H.S.; Borojevic, R. Multicellular spheroids of bone marrow stromal cells: A three-dimensional in vitro culture system for the study of hematopoietic cell migration. *Braz. J. Med. Biol. Res.* **2005**, *38*, 1455–1462. [CrossRef]
10. Wang, W.; Itaka, K.; Ohba, S.; Nishiyama, N.; Chung, U.I.; Yamasaki, Y.; Kataoka, K. 3D spheroid culture system on micropatterned substrates for improved differentiation efficiency of multipotent mesenchymal stem cells. *Biomaterials* **2009**, *30*, 2705–2715. [CrossRef]
11. Zhang, W.; Zhuang, A.; Gu, P.; Zhou, H.; Fan, X. A review of the three-dimensional cell culture technique: Approaches, advantages and applications. *Curr. Stem. Cell Res. Ther.* **2016**, *11*, 370–380. [CrossRef] [PubMed]
12. Guilak, F.; Cohen, D.M.; Estes, B.T.; Gimble, J.M.; Liedtke, W.; Chen, C.S. Control of stem cell fate by physical interactions with the extracellular matrix. *Cell Stem. Cell* **2009**, *5*, 17–26. [CrossRef]
13. Ruedinger, F.; Lavrentieva, A.; Blume, C.; Pepelanova, I.; Scheper, T. Hydrogels for 3D mammalian cell culture: A starting guide for laboratory practice. *Appl. Microbiol. Biotechnol.* **2015**, *99*, 623–636. [CrossRef] [PubMed]
14. Cesarz, Z.; Tamama, K. Spheroid Culture of Mesenchymal Stem Cells. *Stem. Cells Int.* **2016**, *2016*, 9176357. [CrossRef] [PubMed]
15. Hildebrandt, C.; Buth, H.; Thielecke, H. A scaffold-free in vitro model for osteogenesis of human mesenchymal stem cells. *Tissue Cell* **2011**, *43*, 91–100. [CrossRef] [PubMed]
16. Lin, R.Z.; Chang, H.Y. Recent advances in three-dimensional multicellular spheroid culture for biomedical research. *Biotechnol. J.* **2008**, *3*, 1172–1184. [CrossRef] [PubMed]
17. Bierwolf, J.; Lutgehetmann, M.; Feng, K.; Erbes, J.; Deichmann, S.; Toronyi, E.; Stieglitz, C.; Nashan, B.; Ma, P.X.; Pollok, J.M. Primary rat hepatocyte culture on 3D nanofibrous polymer scaffolds for toxicology and pharmaceutical research. *Biotechnol. Bioeng.* **2011**, *108*, 141–150. [CrossRef]
18. Frith, J.E.; Thomson, B.; Genever, P.G. Dynamic three-dimensional culture methods enhance mesenchymal stem cell properties and increase therapeutic potential. *Tissue Eng. Part C Methods* **2010**, *16*, 735–749. [CrossRef] [PubMed]
19. Anghileri, E.; Marconi, S.; Pignatelli, A.; Cifelli, P.; Galie, M.; Sbarbati, A.; Krampera, M.; Belluzzi, O.; Bonetti, B. Neuronal differentiation potential of human adipose-derived mesenchymal stem cells. *Stem Cells Dev.* **2008**, *17*, 909–916. [CrossRef] [PubMed]
20. Zhang, S.; Buttler-Buecher, P.; Denecke, B.; Arana-Chavez, V.E.; Apel, C. A comprehensive analysis of human dental pulp cell spheroids in a three-dimensional pellet culture system. *Arch. Oral Biol.* **2018**, *91*, 1–8. [CrossRef] [PubMed]
21. Lee, S.H.; Inaba, A.; Mohindroo, N.; Ganesh, D.; Martin, C.E.; Chugal, N.; Kim, R.H.; Kang, M.K.; Park, N.H.; Shin, K.H. Three-dimensional Sphere-forming Cells Are Unique Multipotent Cell Population in Dental Pulp Cells. *J. Endod.* **2017**, *43*, 1302–1308. [CrossRef] [PubMed]
22. Yeh, H.Y.; Liu, B.H.; Sieber, M.; Hsu, S.H. Substrate-dependent gene regulation of self-assembled human MSC spheroids on chitosan membranes. *BMC Genom.* **2014**, *15*, 10. [CrossRef] [PubMed]
23. Wong, S.F.; No, D.Y.; Choi, Y.Y.; Kim, D.S.; Chung, B.G.; Lee, S.H. Concave microwell based size-controllable hepatosphere as a three-dimensional liver tissue model. *Biomaterials* **2011**, *32*, 8087–8096. [CrossRef] [PubMed]
24. Lee, S.I.; Ko, Y.; Park, J.B. Evaluation of the maintenance of stemness, viability, and differentiation potential of gingiva-derived stem-cell spheroids. *Exp. Ther. Med.* **2017**, *13*, 1757–1764. [CrossRef]
25. Kim, Y.; Baipaywad, P.; Jeong, Y.; Park, H. Incorporation of gelatin microparticles on the formation of adipose-derived stem cell spheroids. *Int. J. Biol. Macromol.* **2018**, *110*, 472–478. [CrossRef] [PubMed]
26. Lee, S.I.; Ko, Y.; Park, J.B. Evaluation of the osteogenic differentiation of gingiva-derived stem cells grown on culture plates or in stem cell spheroids: Comparison of two- and three-dimensional cultures. *Exp. Ther. Med.* **2017**, *14*, 2434–2438. [CrossRef]
27. Lee, S.I.; Ko, Y.; Park, J.B. Evaluation of the shape, viability, stemness and osteogenic differentiation of cell spheroids formed from human gingiva-derived stem cells and osteoprecursor cells. *Exp. Ther. Med.* **2017**, *13*, 3467–3473. [CrossRef]
28. Lee, S.I.; Yeo, S.I.; Kim, B.B.; Ko, Y.; Park, J.B. Formation of size-controllable spheroids using gingiva-derived stem cells and concave microwells: Morphology and viability tests. *Biomed. Rep.* **2016**, *4*, 97–101. [CrossRef]
29. Jiang, Y.; Pjesivac-Grbovic, J.; Cantrell, C.; Freyer, J.P. A multiscale model for avascular tumor growth. *Biophys. J.* **2005**, *89*, 3884–3894. [CrossRef]
30. Curcio, E.; Salerno, S.; Barbieri, G.; De Bartolo, L.; Drioli, E.; Bader, A. Mass transfer and metabolic reactions in hepatocyte spheroids cultured in rotating wall gas-permeable membrane system. *Biomaterials* **2007**, *28*, 5487–5497. [CrossRef]
31. Mueller-Klieser, W. Method for the determination of oxygen consumption rates and diffusion coefficients in multicellular spheroids. *Biophys. J.* **1984**, *46*, 343–348. [CrossRef]

32. Yamamoto, M.; Kawashima, N.; Takashino, N.; Koizumi, Y.; Takimoto, K.; Suzuki, N.; Saito, M.; Suda, H. Three-dimensional spheroid culture promotes odonto/osteoblastic differentiation of dental pulp cells. *Arch. Oral Biol.* **2014**, *59*, 310–317. [CrossRef] [PubMed]
33. Kikuchi, H.; Suzuki, K.; Sakai, N.; Yamada, S. Odontoblasts induced from mesenchymal cells of murine dental papillae in three-dimensional cell culture. *Cell Tissue Res.* **2004**, *317*, 173–185. [CrossRef] [PubMed]
34. Yamaguchi, Y.; Ohno, J.; Sato, A.; Kido, H.; Fukushima, T. Mesenchymal stem cell spheroids exhibit enhanced in-vitro and in-vivo osteoregenerative potential. *BMC Biotechnol.* **2014**, *14*, 105. [CrossRef] [PubMed]
35. Bellotti, C.; Duchi, S.; Bevilacqua, A.; Lucarelli, E.; Piccinini, F. Long term morphological characterization of mesenchymal stromal cells 3D spheroids built with a rapid method based on entry-level equipment. *Cytotechnology* **2016**, *68*, 2479–2490. [CrossRef]
36. Sart, S.; Tsai, A.C.; Li, Y.; Ma, T. Three-dimensional aggregates of mesenchymal stem cells: Cellular mechanisms, biological properties, and applications. *Tissue Eng. Part B Rev.* **2014**, *20*, 365–380. [CrossRef]
37. Tominaga, H.; Ishiyama, M.; Ohseto, F.; Sasamoto, K.; Hamamoto, T.; Suzuki, K.; Watanabe, M. A water-soluble tetrazolium salt useful for colorimetric cell viability assay. *Anal. Commun.* **1999**, *36*, 47–50. [CrossRef]
38. Ishiyama, M.; Miyazono, Y.; Sasamoto, K.; Ohkura, Y.; Ueno, K. A highly water-soluble disulfonated tetrazolium salt as a chromogenic indicator for NADH as well as cell viability. *Talanta* **1997**, *44*, 1299–1305. [CrossRef]
39. Teo, A.; Mantalaris, A.; Lim, M. Influence of culture pH on proliferation and cardiac differentiation of murine embryonic stem cells. *Biochem. Eng. J.* **2014**, *90*, 8–15. [CrossRef]
40. Amirikia, M.; Ali Jorsaraei, S.G.; Ali Shariatzadeh, S.M.; Mehranjani, M.S. Differentiation of stem cells from the apical papilla into osteoblasts by the elastic modulus of porous silk fibroin scaffolds. *Biologicals* **2019**, *57*, 1–8. [CrossRef]
41. Yan, X.Z.; van den Beucken, J.; Yuan, C.; Jansen, J.A.; Yang, F. Spheroid formation and stemness preservation of human periodontal ligament cells on chitosan films. *Oral Dis.* **2018**, *24*, 1083–1092. [CrossRef] [PubMed]
42. Okumura, K.; Nakamura, K.; Hisatomi, Y.; Nagano, K.; Tanaka, Y.; Terada, K.; Sugiyama, T.; Umeyama, K.; Matsumoto, K.; Yamamoto, T.; et al. Salivary gland progenitor cells induced by duct ligation differentiate into hepatic and pancreatic lineages. *Hepatology* **2003**, *38*, 104–113. [CrossRef] [PubMed]
43. Zhao, S.; Fung-Leung, W.P.; Bittner, A.; Ngo, K.; Liu, X. Comparison of RNA-Seq and microarray in transcriptome profiling of activated T cells. *PLoS ONE* **2014**, *9*, e78644. [CrossRef] [PubMed]
44. Laschke, M.W.; Schank, T.E.; Scheuer, C.; Kleer, S.; Schuler, S.; Metzger, W.; Eglin, D.; Alini, M.; Menger, M.D. Three-dimensional spheroids of adipose-derived mesenchymal stem cells are potent initiators of blood vessel formation in porous polyurethane scaffolds. *Acta Biomater.* **2013**, *9*, 6876–6884. [CrossRef] [PubMed]
45. Xie, H.; Cao, T.; Gomes, J.V.; Neto, A.n.H.C.; Rosa, V. Two and three-dimensional graphene substrates to magnify osteogenic differentiation of periodontal ligament stem cells. *Carbon* **2015**, *93*, 266–275. [CrossRef]
46. Tsai, A.C.; Liu, Y.; Yuan, X.; Ma, T. Compaction, fusion, and functional activation of three-dimensional human mesenchymal stem cell aggregate. *Tissue Eng. Part A* **2015**, *21*, 1705–1719. [CrossRef]
47. Bartosh, T.J.; Ylostalo, J.H.; Bazhanov, N.; Kuhlman, J.; Prockop, D.J. Dynamic compaction of human mesenchymal stem/precursor cells into spheres self-activates caspase-dependent IL1 signaling to enhance secretion of modulators of inflammation and immunity (PGE2, TSG6, and STC1). *Stem Cells* **2013**, *31*, 2443–2456. [CrossRef]